

Trigger - and heat-transfer times measured during experimental molten-fuel-interactions

N. Spitznagel, T. Dürig, and B. Zimanowski

Physikalisch-Vulkanologisches Labor, Universität Würzburg, Pleicherwall 1, 97070 Würzburg, Germany

(Received 15 July 2013; accepted 14 October 2013; published online 23 October 2013)

A modified setup featuring high speed high resolution data and video recording was developed to obtain detailed information on trigger and heat transfer times during explosive molten fuel-coolant-interaction (MFCI). MFCI occurs predominantly in configurations where water is entrapped by hot melt. The setup was modified to allow direct observation of the trigger and explosion onset. In addition the influences of experimental control and data acquisition can now be more clearly distinguished from the pure phenomena. More precise experimental studies will facilitate the description of MFCI thermodynamics. © 2013 Author(s). All article content, except where otherwise noted, is licensed under a Creative Commons Attribution 3.0 Unported License. [<http://dx.doi.org/10.1063/1.4827023>]

When a hot melt gets into direct contact with liquid water, denoted molten fuel coolant interaction (MFCI) can result in vivid explosions. These scenarios occur in accidents, e.g. in metal smelters and power-plants (Chernobyl)¹ or in volcanic eruptions (last famous example Eyafjallajökull 2010).² Hence, in the recent past, experimental studies were performed to explain and to understand MFCI with the aim to improve hazard assessment and risk management as well as to better understand the volcanic ash problem.³⁻⁶ The first aim of these studies was a phenomenological understanding of the process.⁷⁻¹⁰ Therefore it was necessary to reconstruct such explosions under controlled conditions. MFCI-experiments have been performed by a number of working groups,¹¹ using basically three geometrical settings: droplet-experiments, when droplets of hot melt fall into water,^{12,13} layer-experiments, in which a layer of water is superimposed onto a layer of melt¹⁴ and so called entrapment experiments, in which a domain of water is injected into hot melt.^{8,15,16} In this article we present a modified setup for experiments in entrapment configuration.

In all configurations, the process of MFCI can generally be divided into four phases.⁸ The first one is the premix of melt and water. If the temperature of melt is higher than the homogenous nucleation temperature of water (312 °C, at Standard Ambient Temperature and Pressure), a vapour film will establish. This vapour film reduces the heat conduction between melt and water in a range of two magnitudes.^{17,18} In the second phase this vapour film collapses, when triggered by mechanical shock¹⁹ or instability of the vapour film. During the third phase melt and liquid water are in direct contact and the energy transfer takes place. If in a premix of hot melt and coolant under incompressible conditions (hydraulic coupling) the initial interface is large enough to cause a critical thermal flux, the expanding coolant pressurizes the melt beyond its mechanical strength. Ductile-brittle transformation and fragmentation takes place.²⁰ The melt is fragmented by rapid crack propagation and new hot surface is produced with a high rate.²¹ This again increases the heat flux starting an escalating feedback mechanism. The resulting fragments are very small in size and are denoted “ash particles”.^{4,15} The coolant itself transforms into a superheated liquid. Although the time of direct contact is very short, the cooling rate of interactive melt is higher than $10^6 \frac{K}{s}$ and a high amount of energy is transferred. In the last stage the system expands volumetrically, the superheated coolant vaporizes, and decouples the system thermally and hydraulically. In the case of entrapment experiments the fragmentated material is blown out. During the ejection also new ash particles are created by hydrodynamic fragmentation. Studies on the first, second and last stage are

already published in detail.^{9,16,21–23} The most interesting part of this process from the energetical point of view, however, is the third stage, which is characterized by hardly accessible short-time processes at the scale of microseconds.

With the previous setup it was not yet possible to get more detailed information about the third phase. For further investigation of still lacking questions of MFCI (e. g. the influence of melt and water temperature) it is important to get more detailed information of the transition from the second to the third phase and the duration of heat transfer, which take place in a very short time of less than 1 ms. The technical problem is the investigation of the process during the trigger and heat transfer phase in the crucible since no transparent material for the melt and the crucible can be used. In this work we look for a way of indirect acquisition of the required information, which will help us in further experimental studies. There are data missing of the duration of short time phases (duration of vapour film collapse and duration of direct contact between melt and liquid water). The time resolution of the recording system must be as high as possible. One specific task in this work is to get a direct view on the melt surface to observe the time between bullet impact and begin of the expansion of the system. Another task is to have a comparison between the data from the acquisition system (for a start the force signal) and the correspondent state or process in the crucible.

For the presented experiments we used a setup for MFCI entrapment experiments (Figures 1 and 2). The melt is heated in a steel crucible by an inductive heating. Its temperature was measured by a thermocouple. Because of the heterogeneous consistence of the melt the precision of temperature measurement was in the range of $\pm 20 K$. The injection unit can be moved in x- and z-direction, so that the injection tube can be dived into the melt short before the water injection. The linear drive for the piston pump pushes through the thin walled steel tube, if the solenoid is open and water can be merged into the melt for an entrapment experiment. The explosion was triggered by the impact of a low-energy projectile (5 to 6 J) fired from an air-gun onto the surface of the premix. The energy provided by the bullet is much lower than the converted thermal energy in the whole process, which is in the range from 10^2 to $10^4 J$. The force sensor is fixed under the coolant unit on a sandbed. A high speed camera system with a frame rate up to 50,000 pictures per second and a data acquisition system with 100,000 samples per second now enable the observation of short time events during the phase of fine fragmentation. The updated recording system now allows data acquisition and video recording of the experiment in the μs range. Particles were recovered from the Teflon coated containment and consequently analyzed. A mirror was used to record the surface of the melt from above. With this view it is possible to obtain additional information about timing between the projectile impact and the beginning of the 4th phase (blow out). It is also possible to synchronize the process-steps visible in the video with the recorded force-signals. The controlling system and the data acquisition system are completely computerized.

For the presented runs, the following procedure was chosen: When the melt had been heated, the inductive heating was turned off and the injection tube was driven into the melt. A metallic tin melt was used metallic tin melt, as its thermal properties are nearly constant in a wide temperature range.^{21,24} Thus the influence of variation in material properties can be neglected. The data recording system was started at the time as the water injection begun, the recording time was 2 s. A $(7.2 \pm 0.7) ml$ volume of water was injected. In all experimental runs, the injected liquid was at standard room temperature. The pumping time was 440 ms in total, but as the solenoid was opened 100 ms after the start, the actual injection time was 340 ms. At the moment of opening the recording of the high-speed-camera started. The injection velocity was has shown to be in a range from 1.0 to $1.5 \frac{m}{s}$. The bullet in the air gun was launched after 440 ms, i.e. at the moment when the water injection was finished. It took the bullet about 30 to 40 ms until it reached the surface of the melt. At the instant when the bullet hit and disrupted the melt surface, shock waves were generated, propagated with supersonic speed, i.e. with more than $2.5 \cdot 10^3 \frac{m}{s}$ through the melt²⁵ and triggered mechanically the 3rd phase of MFCI.²⁰ Due to these high velocities and supported by results of previous experimental studies,²⁰ it can be assumed that the explosion is always triggered before the bullet penetrates the melt-water layer. After the explosion took place, the camera and the data recording system were stopped, then the injection tube was finally removed.

Figure 3 shows the record of a MFCI run by the high-speed-camera with a frame rate of 20,000 pictures per second. The most important static shots of this video are shown in Figure 4(a)–4(c).

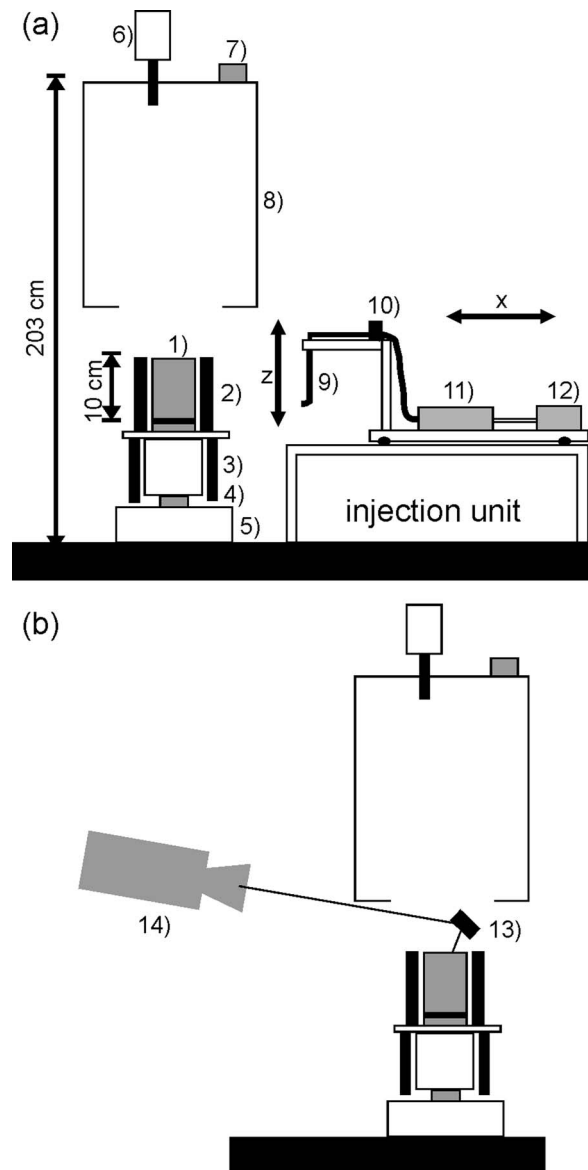


FIG. 1. (a) Schematic of the entrapment setup with its injection unit. 1) Melt crucible within the induction coil 2). The force-sensor 4) is placed under the coolant block 3) on a sandbed 5). The trigger unit 6) is placed above. A seismometer 7) is placed on top of the containment 8). The injection tube 9) can be driven by linear x- and z-stepper motors. The solenoid 10) is placed between the piston pump 11) and the injection tube. The piston pump is driven by a linear stepper motor 12). (b) Side view shows the adjusted mirror 13) to observe the melt surface by the high speed camera 14).

Figure 5(a) displays the typical force signal of an ideal run representing a single triggered explosion. A small peak (1), mostly superposed by a big “main peak” (2). Those pre-cursing small peaks most likely result from the shock waves emitted during brittle fragmentation. The main peak represents the repulsion force on the crucible by the blown out material. In some cases a third peak is visible (3), which is caused by expanding steam. The small peaks later on (4) show the oscillation “ringing” of the crucible after the explosion. It has to be noted that deviations from such “ideal” force signatures were not rare. In some cases there is more than one “main peak”, because multiple explosions occurred. (Figure 5(b)) shows such a run, where three explosions were triggered in a very quick succession, marked by the numbers (1), (2) and (3). If temperature is lower than 600 °C the premature premixes were self-triggered in consequence of the collapse of unstable vapour-film^{12,13} before a

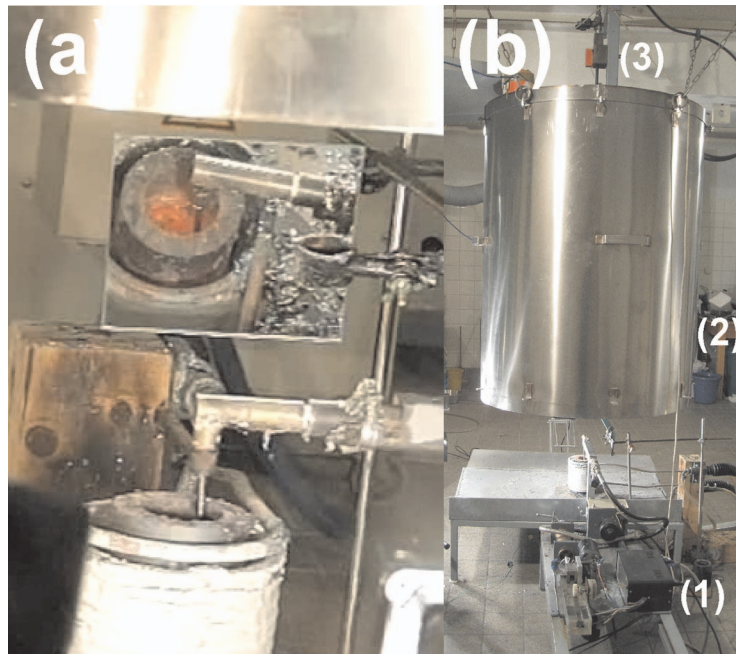


FIG. 2. (a) Melt crucible surrounded by the induction coil. The mirror above allows a direct view onto the melt surface. The injector tube is lowered into the melt for immersed water injection. The containment on the top is for collecting blown out particles. (b) Full experimental setup overview of the setup: (1) water injection unit, (2) containment for particle recovery, (3) solenoid for the trigger gun.



FIG. 3. Video recorded by the high-speed-camera. It shows the complete process of MFCI from bullet impact to the blow out of particles. The frame rate was 20,000 fps. (enhanced online) [URL: <http://dx.doi.org/10.1063/1.4827023.1>].

mechanical collapse could be initialized by the bullet (Figure 5(c), Peak (1)). In cases of higher temperatures, however, the collapse had to be forced mechanically. External triggering is preferred for MFCI investigations, as the resulting intensity of the explosive interaction is higher than in the case of self-triggering.¹⁰

By means of the adjusted mirror, it can be observed that the time between trigger (bullet impact) and the opening of the system was shorter than 1 ms in all runs, but with variations between 250 μ s and 900 μ s. If the premix is in an agitated state, that means that there is a tremor motion during the premix, this period will be significantly shorter, which suggests that in such cases the vapour



FIG. 4. Frame of high-speed recording of an MFCI-run. 150 ml of tin melt were heated on 900 °C. The frame rate was 20,000 fps. At $t = 0$ ms the water injection pump is started, after 100 ms the solenoid opens and the video recording is started. It ends after $t = 440$ ms and the trigger projectile is launched from the gun. 40.05 ms later it arrives at the melt surface ($t = 480.05$ ms, frame 7601, picture (a)). At $t = 480.75$ ms (frame 7615) the melt surface breaks up, picture (b). At frame 7660 at $t = 483.00$ ms (picture (c)) the recorded force signal is maximum (see Figure 4). Some ash particles leave the system around the injection tube. The video linked to Figure 3 shows the complete process.

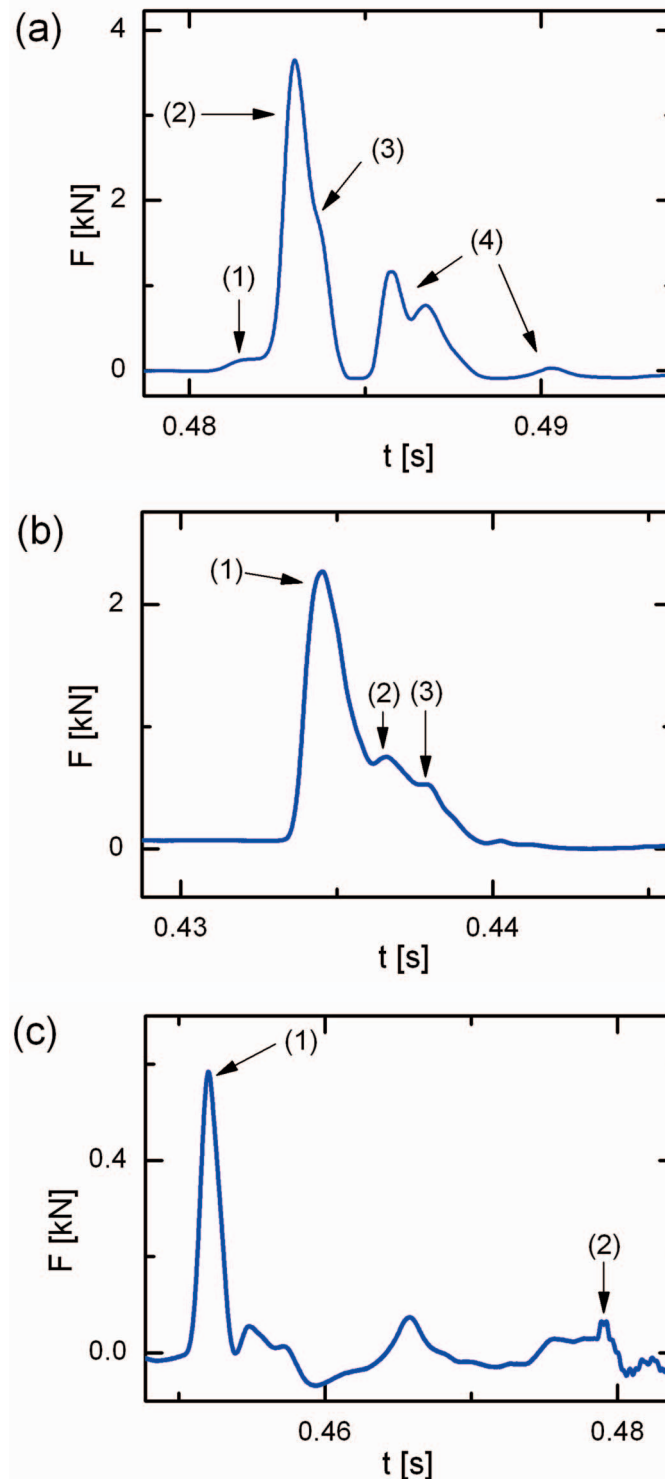


FIG. 5. Force signals during MFCI explosions. (a) A signal of a single explosion. This is the force-signal from the explosion presented in Fig. 2 and 3. (1) shows the transmitted signal from shockwaves, (2) the “main peak” represents the acceleration for blowout, (3) the steam expansion and (4) the “ringing” of the crucible after the explosion. (b) A multiple triggered run, numbers (1–3) shows the “main peaks” of the three single explosions in very quick successions. The melt volume was 70 ml, the melt temperature was 900 °C and the injected water volume was only about 5 ml with an injection time of 400 ms in this run. (c) A self triggered explosion (1). (2) represents the impact of the projectile after spontaneous self triggering. The volume was 70 ml, the melt temperature 400 °C.

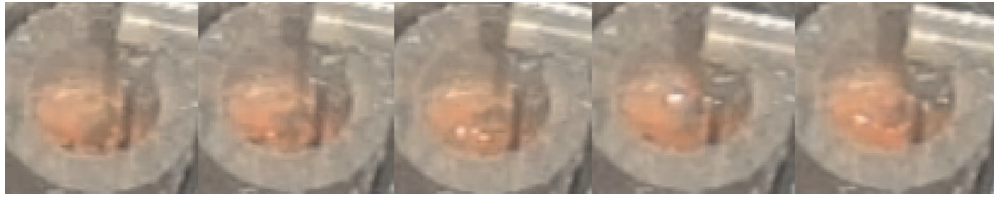


FIG. 6. Some shots during the injection of water. The different bright spots in the images show the locations, where agitated melt reflects light. The melt temperature in this run was 900 °C, the crucible was filled with 70 ml of tin.

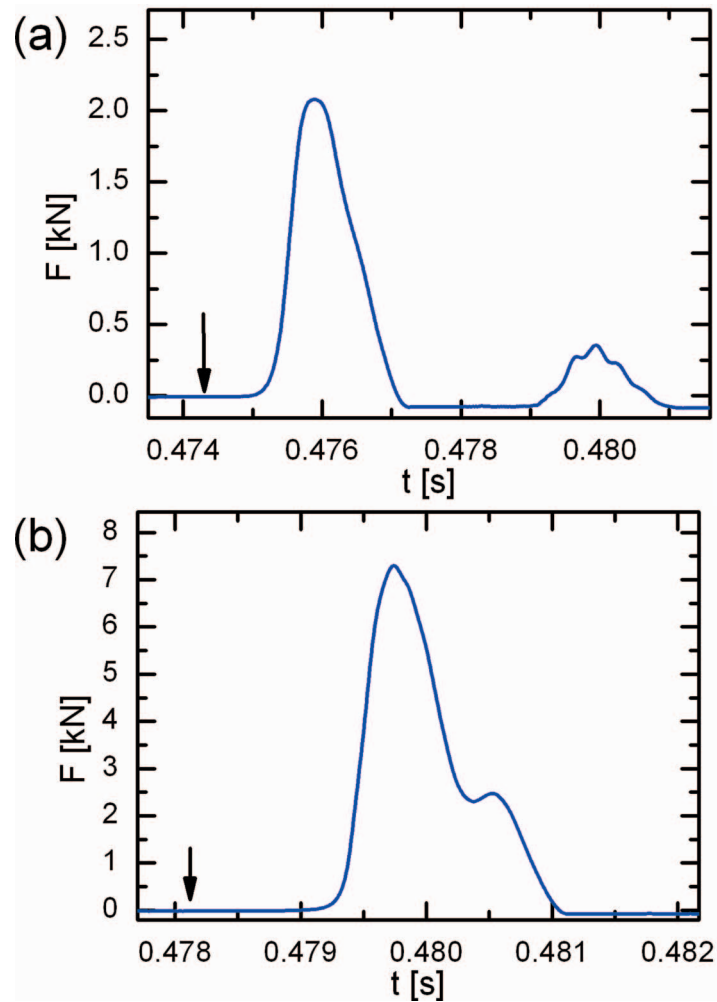


FIG. 7. Effect on propagation of the force signal. The arrows show the moment of projectile impact contained by the video analysis. (a) Single triggered explosion. The time between impact and begin of expansion is 700 μ s seen in the video (70 ml of tin at 900 °C). (b) Double explosion (70 ml of tin at 900 °C). The time between impact and begin of the force peak is longer, although the time according to the video is only 250 μ s. This delay can be explained by the fact that the seismic signal has to pass several melt-water interfaces, before being detected by the force sensor.

collapses occur faster or the water droplet is more close to the melt surface. With this information we can conclude that the pure time of direct contact between melt and liquid water (i.e. after the collapse and until the end of fragmentation) is shorter than 0.5 ms.

It is interesting to analyze the state of the melt in the crucible at the moment when the force reaches its peak. It turns out that at this moment the melt surface is breaking up and sometimes first

particles leave the system (Figure 4(c)). It can be concluded, that the acceleration of the blown out material is maximal at this time.

If the system is agitated (tremor) during premix, the probability for multiple-triggering was observed to be higher. An explanation for this effect might be, that in the agitated system multiple water-domains are established (Figure 6). After triggering the first domain, the others are triggered in a chain reaction by the mechanical shock waves generated from exploding pervious ones.

A more detailed comparison between the recorded force-signal and the video analysis shows that the transmission time from the centre of event in the crucible to the force transducer depends on the individual melt water mix. The transmission time is longer for the first force peak in multiple triggered experiments (Figure 7). Additionally in those cases the time until the breakup at the surface is shorter, because of the shorter distance from high levelled domains to the surface of the melt.

In future MFCI entrapment experiments the improvements on the setup such as a higher time resolution, influences of the premix on the whole process, the duration of trigger and heat transfer and a better comparison from the recorded force signal with the state in the melt-water-system will allow a better understanding of details of the short-term processes.

ACKNOWLEDGMENTS

We thank the unknown reviewers for their valuable comments and helpful suggestions.

- ¹E. E. Purvis, *The Chernobyl 4 accident sequence: update-April 1995* (ISTC, Kiev, 1995).
- ²V. Lorenz, *Chem. Geol.* **62**, 149–156 (1987).
- ³K. H. Wohletz, *J. Volcanol. Geotherm. Res.* **17**, 31–64 (1983).
- ⁴B. Zimanowski, K. H. Wohletz, P. Dellino, and R. Büttner, *J. Volcanol. Geotherm. Res.* **2557**, 1–5 (2002).
- ⁵A. Hall, *Nuclear Engineering and Design* **109**, 407–415 (1988).
- ⁶A. Freud, R. Harari, and E. Sher, *Nuclear Engineering and Design* **239**(4), 722–727 (2009).
- ⁷G. Fröhlich and A. Schatz, *Dampfexplosion: Das unerklärte Phänomen – Unfallanalysen/Vulkanismus/Metallurgie*, Jahrbuch Univ. Stuttgart 1994, 73–84, Stuttgart, 1995.
- ⁸R. Büttner and B. Zimanowski, *Phys. Rev. E* **57**, 5726–5729 (1998).
- ⁹G. Fröhlich, B. Zimanowski, V. Lorenz, B. Bayer, E. v. Berg, M. Khan, and M. Schindler, *Experimente zur Simulation phreatomagmatischer Explosionen und vergleichende Untersuchungen, Abschlussbericht*, 1992.
- ¹⁰G. Fröhlich, B. Zimanowski, V. Lorenz, *Explosive thermal interactions with molten lava and water 1993: Proc 3rd World Conf on Fluid Mechanics and Thermodynamics*, Honolulu, Hawaii (Elsevier, Amsterdam, 1993), 1459–1468.
- ¹¹Double issue of Nuclear Engineering and Design on fuel-coolant interactions and steam explosions, *Nucl. Eng. Des.* **155**, 1–2 (1995).
- ¹²G. Fröhlich, *Chem.-Ing.-Tech.* **50**(11), 861–866 (1978).
- ¹³T. Li, Y. Yang, M. Yuan, and Z. Hu, *Nuclear Science and Techniques* **18**(5), 311–315 (2007).
- ¹⁴A. Austin-Erickson, R. Büttner, P. Dellino, M. H. Ort, and B. Zimanowski, *J. Geophys. Res.* **113**, B11201, doi:10.1029/2008JB005731 (2008).
- ¹⁵R. Büttner, B. Zimanowski, C. O. Mohrholz, and R. Kümmel, *Journal of Applied Physics* **98**, 043524-1–043524-8 (2005).
- ¹⁶B. Zimanowski, R. Büttner, and V. Lorenz, *Bull Volcanol* **58**, 491–495 (1997).
- ¹⁷L. A. Bromley, *Chem. Eng. Prog.* **46**, 221–227 (1950).
- ¹⁸R. B. Duffy, *Int. J. Heat Mass Transfer* **16**, 1513–1525 (1973).
- ¹⁹D. F. Fletcher, *Nucl. Eng. Des.* **155**, 27–36 (1995).
- ²⁰B. Zimanowski, R. Büttner, and J. Nestler, *Europhys. Lett.* **38**(4), 285–289 (1997).
- ²¹A. Fagents, T. K. P. Gregg, and R. M. C. Lopes, *Modelling Volcanic processes, The Physics and Mathematics of Volcanism*, Chapter 11, (Cambridge University Press, 2013).
- ²²B. Zimanowski, G. Fröhlich, and V. Lorenz, *J. Volcanol. Geotherm. Res.* **48**, 341–358 (1991).
- ²³B. Zimanowski, V. Lorenz, and G. Fröhlich, *J. Volcanol. Geotherm. Res.* **30**, 149–153 (1986).
- ²⁴R. Büttner, B. Zimanowski, J. Blumm, and L. Hagemann, *J. Volcanol. Geotherm. Res.* **80**, 293–302 (1998).
- ²⁵L. Calderín, D. J. Gonzales, L. E. Gonzalez, and J. M. López, *J. Chem. Phys.* **129**, 194506 (2008).